Kinetics of the Reductive Half-Reaction of the Iron−Sulfur Flavoenzyme CDP-6-deoxy-L-*threo*-D-*glycero*-4-hexulose-3-dehydrase Reductase†

George T. Gassner,‡ David A. Johnson,§ Hung-wen Liu,*,§ and David P. Ballou*,‡

Department of Biological Chemistry, University of Michigan, Ann Arbor, Michigan 48109-0606, and Department of Chemistry, University of Minnesota, Minneapolis, Minnesota 55455

Received January 29, 1996; Revised Manuscript Received April 5, 1996⊗

ABSTRACT: The conversion of CDP-4-keto-6-deoxy-D-glucose to CDP-4-keto-3,6-dideoxy-D-glucose is a key step in biosynthesis of ascarylose, the terminal dideoxyhexose of the *O*-antigen tetrasaccharide of the lipopolysaccharide from *Yersinia pseudotuberculosis V*. This transformation is catalyzed by two enzymes: CDP-6-deoxy-L-*threo*-D-*glycero*-4-hexulose-3-dehydrase (E_1), which contains a pyridoxamine and a [2Fe-2S] center, and an NADH-dependent CDP-6-deoxy-L-*threo*-D-*glycero*-4-hexulose-3-dehydrase reductase (E_3), which contains both an FAD and a [2Fe-2S] center. E_1 reacts to form a Schiff base with CDP-4-keto-6-deoxy-D-glucose and catalyzes the elimination of the hydroxyl at position 3 of the glucose moiety, resulting in the formation of a covalently bound CDP-6-deoxy-$\Delta^{3,4}$-glucoseen intermediate. E_3 transfers electrons from NADH to E_1, which uses these to reduce the $\Delta^{3,4}$-glucoseen bond to produce CDP-4-keto-3,6-dideoxy-D-glucose. In this work, we have investigated the reductive half-reaction of E_3 using both single wavelength and diode array stopped flow absorbance spectroscopy. We find that NADH binds to both oxidized ($K_d = 52.5 \pm 2$ μM) and two-electron-reduced ($K_d = 12.1 \pm 1$ μM) forms of E_3. Hydride transfer from NADH to the FAD moiety occurs at 107.5 ± 3 s^{-1} and exhibits a 10-fold deuterium isotope effect when (4*R*)-[^{2}H]NADH is substituted for NADH. Following the hydride transfer reaction, NAD^+ is released at 42.5 ± 1 s^{-1} and electron transfer from the reduced FAD to the [2Fe-2S] center occurs rapidly. The extent of the intramolecular electron transfer reaction is pH-dependent with a pK_a of 7.3 ± 0.1, which may represent the ionization state of the N-1 position of the FAD hydroquinone of E_3. Finally, E_3 is converted to the three-electron-reduced state in a slow disproportionation reaction that consumes NADH. The [2Fe-2S] center of E_3 was selectively disassembled by titration with mersalyl to give E_3(apoFeS). The properties of this form of the enzyme are compared to those of the holoenzyme. Similarities and differences of the reductive half-reactions of E_3 and related iron−sulfur flavoenzymes are discussed.

Five unusual dideoxyhexoses (abequose, ascarylose, colitose, paratose, and tyvelose) have been isolated from the membranes of Gram-negative bacteria (Lindberg, 1990; Griffiths & Davies, 1991a,b; Matsuhashi *et al*., 1966). These sugars are localized in the *O*-antigen component of the lipopolysaccharide (LPS),[1] where they serve as key antigenic determinants in the immune response to invasive microorganisms (Lüderitz *et al*., 1966). CDP-glucose (**2** in Scheme 1) or GDP-mannose is the starting material for the biosynthesis of all of these sugars, which is thought to proceed through a common 4-keto-3,6-dideoxy-D-hexose intermediate (**9**) (Grisebach, 1978; Shibaev, 1986; Gonzalez-Porqúe & Strominger, 1972; Yu *et al*., 1992). Subtle differences in the subsequent reactions result in the five unique nucleotidyl dideoxyhexoses that are used later in the construction of the *O*-antigen (Health & Elbein, 1962; Matsuhashi *et al*., 1966; Liu & Thorson, 1994; Kessler *et al*., 1993).

CDP-ascarylose (**11**) is the precursor of the nonreducing terminal ascarylose, in the *O*-antigen tetrasaccharide of *Yersinia pseudotuberculosis V* (Ovodov *et al*., 1992). It is synthesized from CDP-glucose (**1**) in a pathway that includes an unusual NADH-dependent deoxygenation of CDP-4-keto-6-deoxy-D-glucose to form CDP-4-keto-3,6-dideoxy-D-glucose (**9**) (Rubenstein & Strominger, 1974a,b; Liu & Thorson, 1994). This reaction is catalyzed by two enzymes: CDP-6-deoxy-L-*threo*-D-*glycero*-4-hexulose-3-dehydrase (E_1) and CDP-6-deoxy-L-*threo*-D-*glycero*-4-hexulose-3-dehydrase reductase[2] (E_3). E_1 is a 49 kDa monomeric enzyme that contains a pyridoxamine 5′-phosphate (PMP) and a [2Fe-2S] center (Weigel *et al*., 1992a,b; Thorson & Liu, 1993a). It catalyzes the formation of a Schiff base between PMP and C-4 of the 4-keto-6-deoxyglucose (**3**)

† Supported by a U.S. Public Service Grant GM 20877 to D.P.B. and a NIH Grant GM35906 to H.-w.L. H.-w.L. is a recipient of a NIH Research Career Development Award (GM00559). D.A.J. is a recipient of a NIGMS Biotechnology Traineeship (2 T32 GM08347).

* To whom correspondence should be addressed at Department of Chemistry, University of Minnesota, Minneapolis, MN 55455, or Department of Biological Chemistry, University of Michigan, Ann Arbor, MI 48109-0606.

‡ University of Michigan.

§ University of Minnesota.

⊗ Abstract published in *Advance ACS Abstracts,* May 15, 1996.

[1] Abbreviations: 5-dRFl, 5-deazariboflavin; CAPS, (cyclohexylamino)propanesulfonic acid; CDP, cytidine 5′-diphosphate; E_1, CDP-6-deoxy-L-*threo*-D-*glycero*-4-hexulose-3-dehydrase; E_3, CDP-6-deoxy-L-*threo*-D-*glycero*-4-hexulose-3-dehydrase reductase; FAD_{hq}, hydroquinone flavin adenine dinucleotide; FAD_{ox}, oxidized flavin adenine dinucleotide; FAD_{sq}, semiquinone flavin adenine dinucleotide; FNR, ferredoxin NADP reductase; LPS, lipopolysaccharide; MES, 2-(*N*-morpholino)-ethanesulfonic acid; MOPS, 3-(*N*-morpholino)propanesulfonic acid; NAD^+ (NADH), nicotinamide adenine dinucleotide (reduced form); NADD, (4*R*)-[^{2}H]nicotinamide adenine dinucleotide; PCA, protocatechuate; PCD, protocatechuate 3,4-dioxygenase; PMP, pyridoxamine 5′-phosphate; TMADH, trimethylamine dehydrogenase; TRIS, tris-(hydroxymethyl)aminomethane; [2Fe-2S], plant-type ferredoxin iron−sulfur center.

S0006-2960(96)00217-6 CCC: $12.00

Scheme 1: Biosynthesis of CDP Ascarylose from Glucose 1-Phosphate and CTP[a]

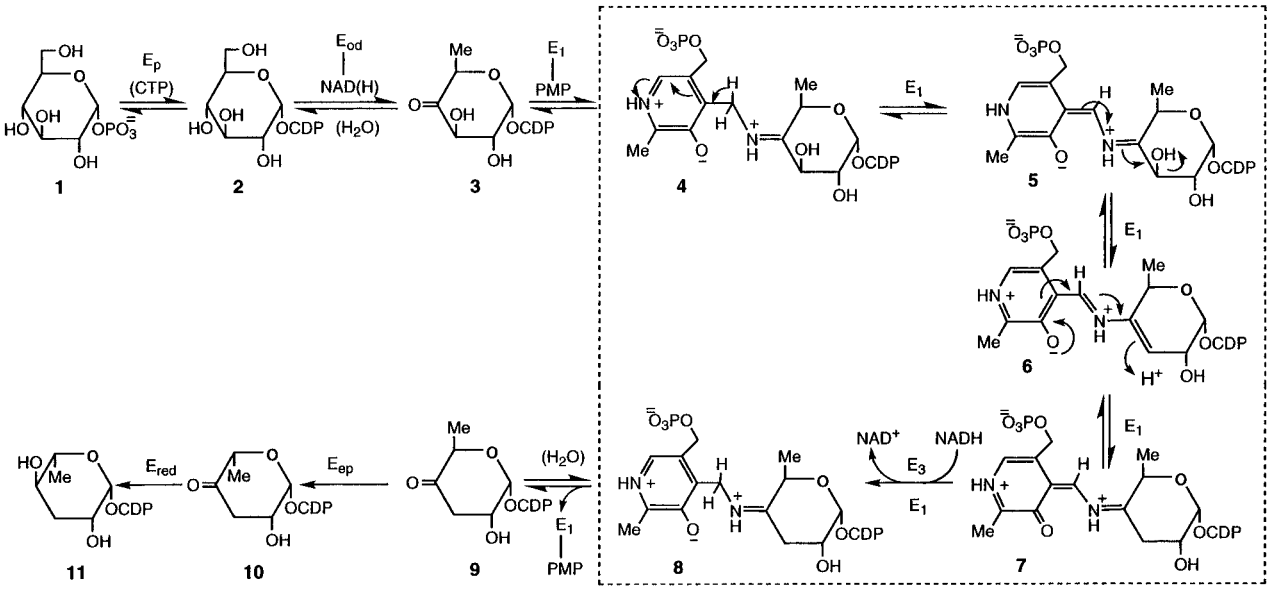

[a] The reactions enclosed in the dashed box are catalyzed by the E_1-E_3 system.

substrate. As shown in Scheme 1, this is followed by a 1,4 dehydration to form a $\Delta^{3,4}$-glucoseen intermediate (**6**). E_3 is a 39 kDa monomeric [2Fe-2S]- and FAD-containing reductase (Miller *et al*., 1993; Lo *et al*., 1994). It accepts a hydride from NADH and transfers two electrons stepwise to E_1 where they are used to reduce the CDP-6-deoxy-$\Delta^{3,4}$-glucoseen intermediate to give CDP-4-keto-3,6-dideoxy-D-glucose. It is proposed that reduction of CDP-6-deoxy-$\Delta^{3,4}$-glucoseen proceeds via a radical mechanism (Thorson & Liu, 1993b), since the electron equivalents used in this reaction are transmitted from the reductase to the dehydrase sequentially through iron centers, which are limited to single electron transfer.

In this paper, stopped flow absorbance spectroscopy is employed in the investigation of the reductive half-reaction of the iron−sulfur flavoenzyme E_3 with NADH. The results of these studies are discussed and compared with related electron transferases.

MATERIALS AND METHODS

E_3 was expressed in *Escherichia coli* strain JM105 containing the pOPI plasmid and purified, with minor modifications, as described previously (Ploux *et al*., 1995). The modifications were as follows. (1) Buffer A was 20 mM TRIS-HCl (pH 7.5), 1 mM β-mercaptoethanol, and 0.1 mM EDTA. (2) The enzymatically active fractions after the DEAE-Sepharose step were pooled and concentrated using an Amicon ultrafiltration unit (YM-10). (3) The MonoQ FPLC purification utilized a flow rate of 3 mL/min and a linear gradient from 0.16 to 0.36 M NaCl in 12 min following a 1 min wash in the absence of NaCl.

E_3(apoFeS) was prepared by titrating 0.16 μmol of E_3 (5.6 mg) with 64 equiv of mersalyl (Aldrich, Milwaukee, WI) in 20 mM TRIS-HCl (pH 8.0) and incubating for 30 min. After concentration of the enzyme using a Centricon 10 concentrator (Amicon, Beverly, MA), excess mersalyl was removed by gel filtration over a disposable Sephadex G-10 column (1 × 5 cm, Bio-Rad Laboratories, Hercules, CA) with 50 mM potassium phosphate (pH 7.5). The protein solution (2.8 mL) was treated with 15 μL of β-mercaptoethanol and allowed to incubate for about 20 min. This mixture was purified on a different Sephadex G-10 column using the same buffer. E_3 irreversibly lost FAD during the course of this preparation such that only a low yield of E_3(apoFeS) could be obtained. Attempts to reconstitute E_3(apoFeS) with FAD were unsuccessful. The final concentration was about 11.5 μM (based on $\epsilon_{454,FAD} = 11\,900\ M^{-1}\ cm^{-1}$).

Single mixing stopped flow studies of the deuterium isotope effect were performed with a Kinetic Instruments, Inc., stopped flow spectrophotometer configured for photomultiplier tube (PMT) detection as described by Gassner *et al*. (1994). A Hi-Tech SF-61 stopped flow spectrophotometer configured for both PMT detection and diode array detection [described previously by Gassner and Ballou (1995)] was employed in all other single mixing stopped flow studies. The pH jump studies were performed using an Applied Photophysics Laboratories stopped flow instrument configured for double mixing.

MES, MOPS, TRIS, and CAPS buffers used in these studies were from Sigma (St. Louis, MO). Phosphate was from Mallinckrodt (Paris, KY). Grade II NAD^+ (98%) and grade I NADH (100%) were from Boehringer Mannheim (Indianapolis, IN). NADD was prepared enzymatically from NAD^+ using a previously described method (Gassner *et al*., 1994).

Programs used for fitting and simulation of kinetic data [as described in Gassner *et al*. (1994, 1995)] were Program A (developed in the Ballou laboratory), KISS software (Kinetic Instruments, Inc.), HopKINSIM [1990 version adapted by D. Wachstock from the KINSIM program of Barshop *et al*. (1983) and Zimmerelle and Frieden (1989)], and Specfit (Spectrum Software Associates, 1993). All stopped flow reactions included 1 μM PCD and 100 μM PCA for maintaining anaerobic conditions (Bull & Ballou, 1981). The Applied Photosystems stopped flow instrument

[2] This enzyme (E_3) has been previously called CDP-6-deoxy-$\Delta^{3,4}$-glucoseen reductase. Realizing that the function of E_3 is actually to transfer electrons to CDP-6-deoxy-L-*threo*-D-*glycero*-4-hexulose-3-dehydrase (E_1), we now refer to it as CDP-6-deoxy-L-*threo*-D-*glycero*-4-hexulose-3-dehydrase reductase.

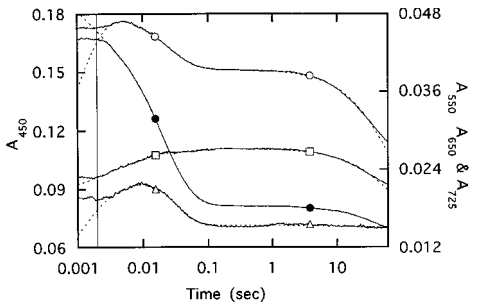

FIGURE 1: Wavelength dependence of the reduction reaction. Reaction of 7.8 μM E_3 with 506 μM NADH at 4 °C in 100 mM TRIS buffer at pH 8.0. Reaction monitored at (●) 450 nm, (○) 550 nm, (□) 650 nm, and (△) 725 nm. Dashed lines are fits to the data. The solid vertical line indicates the stop of flow.

required more stringent preparations in order to ensure anaerobic conditions, since the polyethylene tubing used in this instrument is oxygen permeable. This instrument was prepared as follows. All syringes, tubing, and valves were first filled with 5 mM sodium dithionite in 100 mM phosphate buffer and allowed to sit for 4 h to scrub out oxygen. Just prior to the experiment, the dithionite was replaced with an anaerobic solution containing 100 μM PCA and 1 μM PCD. Finally, this PCA and PCD solution was replaced with the enzyme, NADH, and buffer solutions used in the pH jump study, which also contained PCA and PCD.

Photoreductions (Massey & Hemmerich, 1977, 1978) were performed by irradiating samples with a 650 W tungsten−halogen Sun Gun (Smith-Victor Co.). These reactions were carried out under an argon atmosphere in anaerobic cuvettes containing 100 mM MOPS (pH 7.0) or CAPS buffer (pH 10.0), 5 mM EDTA, and 50 nM 5-dRFl in a H_2O bath at 4 °C. Visible absorbance spectra were recorded periodically using a Cary 3E spectrophotometer in order to monitor the extent of the reduction.

RESULTS

Reaction of E_3 with NADH. Absorbance changes occurring at four different wavelengths in the reaction of E_3 with 506 μM NADH are presented in Figure 1. Analysis of these data allowed us to identify steps of NADH binding, hydride transfer, and NAD^+ release. The NADH binding reaction occurs in the first 5 ms and causes a slight decrease in absorbance between 400 and 500 nm and an increase in absorbance at wavelengths greater than 520 nm that are indicative of the formation of a charge transfer complex of NADH and oxidized FAD. Subsequently (out to ~10 ms), there are decreases in absorbance at 450 and 550 nm and further increases in absorbance at 650 and 725 nm that are consistent with FAD reduction and the formation of a second charge transfer complex between NAD^+ and reduced flavin anion. The third phase of the reaction (out to ~30 ms) is seen as decreases in absorbance at 450, 550, and 725 nm and a slight increase in absorbance at 650 nm, and these changes continue in the fourth phase of the reaction (out to ~100 ms). The loss of charge transfer absorbance ($FAD_{hq} \rightarrow NAD^+$) at 725 nm marks the release of NAD^+ from the enzyme. A decrease in absorbance at 450 and 550 nm occurs as the [2Fe-2S] center is reduced. At 650 nm, the increase in absorbance due to the formation of flavin semiquinone is slightly greater than the decrease in absorbance due to the dissociation of NAD^+ from the ($FAD_{hq} \rightarrow NAD^+$) charge

Scheme 2: Mechanism of the Reductive Half-Reaction of E_3 with NADH[a]

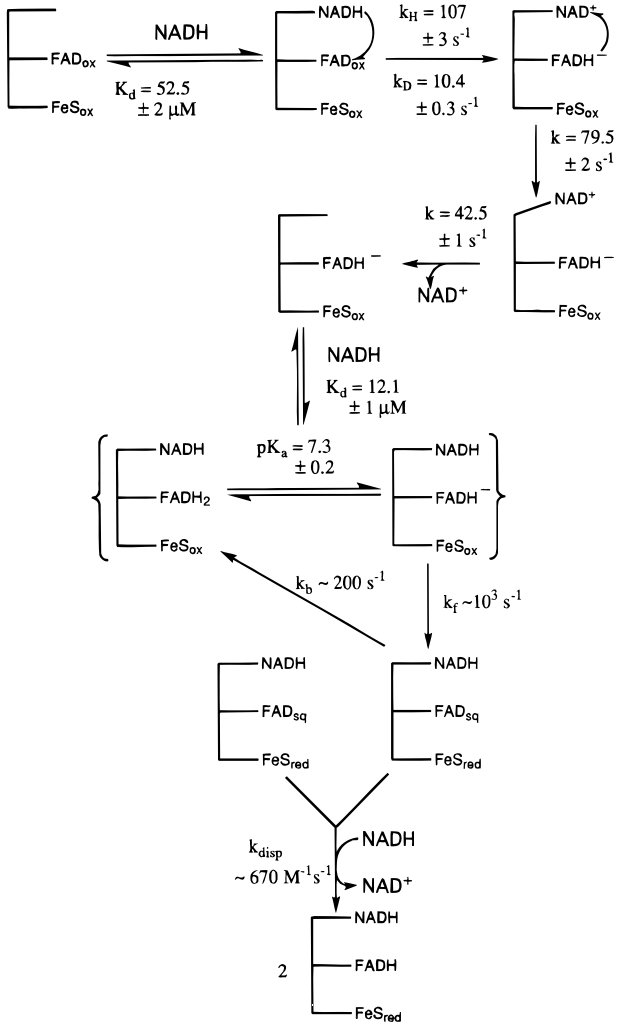

[a] Stick diagrams represent intermediate forms of E_3 involved in the reduction reaction. Rate and equilibrium constants are derived from the experiments described in the text.

transfer complex and reduction of the [2Fe-2S] center, resulting in a net increase in absorbance. In the last phase of the reaction (out to ~100 s), the absorbance at 450, 550, and 650 nm decreases as the enzyme is slowly converted to the three-electron-reduced state as it reacts with excess NADH.

Concentration Dependence of the Reaction of E_3 with NADH. Data from the concentration dependence of the reduction reaction could be fit with a consecutive model containing a minimum of five exponentials (see the first four steps and last step in Scheme 2). The observed rate associated with the first step of the reaction increases linearly with NADH concentration and represents the binding of NADH to oxidized E_3 to form the NADH → FAD_{ox} charge transfer complex (Figure 2) ($K_d = 52.5 \pm 2$ μM; $k_{on} = 1.98 \times 10^6$ M^{-1} s^{-1}; $k_{off} = 103.9$ s^{-1}). Following this initial binding step, hydride is transferred from NADH to the FAD moiety (107.5 ± 3 s^{-1}), resulting in flavin reduction and the formation of a charge transfer complex of flavin hydroquinone and NAD^+. This phase of the reaction is seen as an increase in absorbance in the 700−800 nm region (charge transfer complex formation) and as a larger decrease in absorbance in the 400−500 nm region (FAD reduction) (Figures 1 and 2A). After the hydride transfer reaction, the

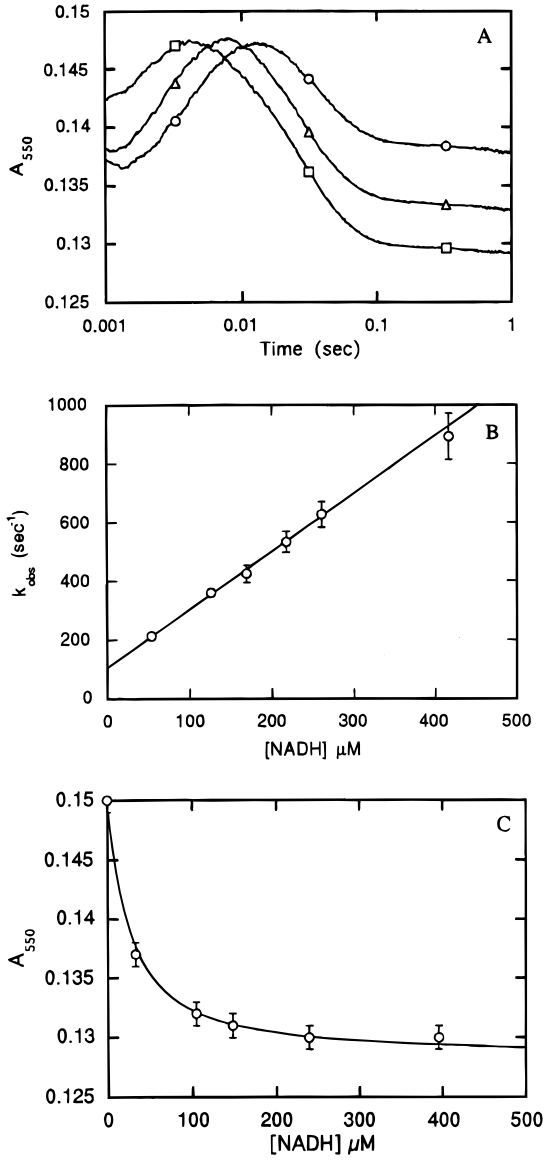

FIGURE 2: Concentration dependence of the reaction of E_3 with NADH. (A) Reaction of 21 μM E_3 with (○) 54 μM, (△) 169 μM, and (□) 417 μM NADH at 4 °C in 50 mM phosphate buffer at pH 7.5. (B) Dependence on NADH concentration of the first observed reaction rate calculated from exponential fits to the data presented in panel A. (C) Hyperbolic decrease at 550 nm due to the binding of excess NADH to two-electron-reduced E_3 during the reduction reaction.

enzyme isomerizes (79.5 ± 2 s^{-1}) and then NAD^+ is released from the reduced enzyme at 42.5 ± 1 s^{-1}. These last two steps are characterized by the loss of flavin hydroquinone to NAD^+ charge transfer absorbance (see absorbance decreases at 550 and 725 nm in Figure 1). As NAD^+ is released from the two-electron-reduced enzyme, free NADH binds tightly to the coenzyme binding site. The complex of two-electron-reduced E_3 and NADH has lower absorbance at 550 nm than free two-electron-reduced E_3 (see Figure 2C and the data in Figure 2A between 100 ms and 1 s). The absorbance of two-electron-reduced E_3 and its complex with NADH (calculated from sequential exponential fits through NADH concentration dependence data collected at 550 nm) is hyperbolically related to the total concentration of NADH remaining following the hydride transfer reaction (see Figure 2C). The dissociation constant of the NADH−E_3 complex was estimated by fitting the data to the ligand binding

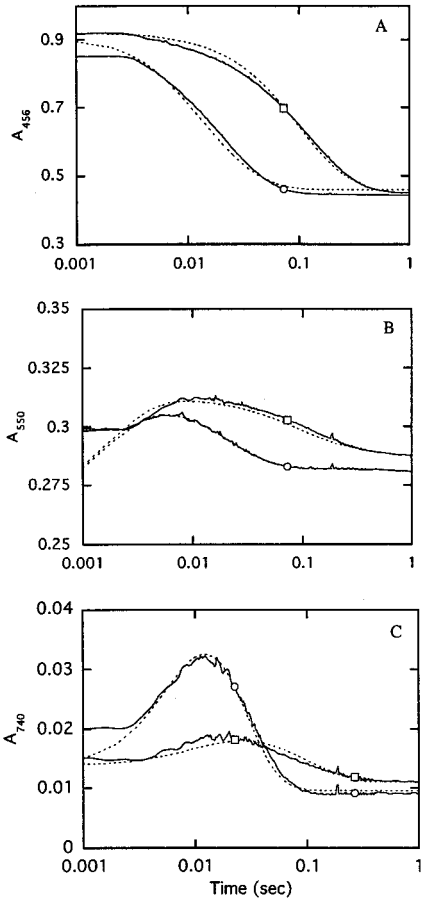

FIGURE 3: Deuterium isotope effect on hydride transfer. Kinetics of the reaction of 40 μM E_3 with 245 μM (○) NADH or (□) NADD at 4 °C in 20 mM TRIS buffer at pH 8.0. Solid lines are the observed data; dotted lines are simulations of the data assuming the model shown in Scheme 1.

equation (eq 1).

$$A = \left[\left[E_3 + \mathrm{NADH_T} + K_d - \sqrt{(E_3 + \mathrm{NADH_T} + K_d)^2 - 4E_3\mathrm{NADH_T}}\right]/2E_3\right]A_T + A_0 \quad (1)$$

The dependent variable A represents the enzyme absorbance at 550 nm at any NADH concentration. A_T is the total enzyme absorbance at 550 nm when the NADH concentration is saturating. A_0 is the constant background enzyme absorbance. E_3 is the total concentration of E_3. $NADH_T$ is the total NADH concentration. K_d is the equilibrium dissociation constant for the E_3−NADH complex. The best fit through the data at 550 nm gives $K_d = 12 \pm 1$ μM with a maximum absorbance change (A_T) of 0.021 ± 0.003 (Figure 2C).

Deuterium Isotope Effect on Hydride Transfer. Binding of NADH to E_3 poises the system for hydride transfer from NADH to the FAD moiety with *pro-R* stereoselectivity (Han *et al*., 1990); the change in the reduction kinetics that occurs upon the substitution of (4*R*)-[^{2}H]NADH (NADD) for NADH was used to identify the second observed phase of the reaction as being representative of hydride transfer (see Figure 3). The initial NADH binding step is followed by a 107.5 s^{-1} reaction characterized by a 8 mM^{-1} cm^{-1} decrease in enzyme extinction at 456 nm, a 0.3 mM^{-1} cm^{-1} decrease at 550 nm, and a 1.1 mM^{-1} cm^{-1} increase at 740 nm (Figure 4). These changes are consistent with FAD reduction and

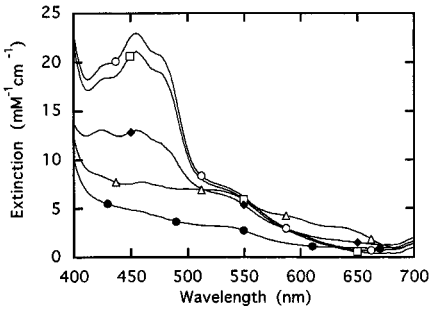

FIGURE 4: Spectra of the major intermediates occurring in the reductive half-reaction of E_3. Spectra were derived through global Marquardt fitting of the diode array data collected during the reaction of 40 μM E_3 with 245 μM NADD or NADH in 20 mM TRIS buffer at pH 8.0. The displayed spectra are most representative of (○) oxidized E_3, (□) the NADH and FAD charge transfer complex, (◆) the NAD^+ and FAD_{hq} charge transfer complex, (△) NADH bound to the reduced iron−sulfur and neutral flavin semiquinone form of E_3, and (●) three-electron-reduced E_3.

the conversion of a charge transfer complex between NADH and FAD into a charge transfer complex between NAD^+ and FAD_{hq}. Data from the reaction of E_3 with NADD could be simulated closely by decreasing the 107.5 s^{-1} rate constant to 10.4 s^{-1} and otherwise using the same intermediate extinctions and reaction rates that gave the best fits to the NADH data (Figure 3). Charge transfer complexes of NADH and FAD have greater absorbance at 550 nm and lesser absorbance at 740 nm than do charge transfer complexes of FAD_{hq} and NAD^+ (Batie & Kamin, 1984; Gassner *et al*., 1994; Gassner & Ballou, 1995). Thus, substitution of NADD for NADH selectively decreases the rate constant associated with hydride transfer and results in greater accumulation of the FAD and NADH-type charge transfer complex. This would have the effect of elevating the transient absorbance observed at 550 nm and depressing the transient absorbance observed at 740 nm. These trends are in fact observed in the data (see Figure 3), so it can be concluded that the second observed phase in the reductive half-reaction of E_3 with NADH represents hydride transfer.

Diode array spectra were recorded during the reactions of E_3 with NADH and with NADD. These data were fit globally using the Marquardt−Levenberg routine built into the program Specfit (Spectrum Software Associates, 1993). The spectra resolved by this fitting procedure, presented in Figure 4, are reasonable representations of the intermediate species involved in the reduction reaction. The composition of these species is shown in the stick diagrams in Scheme 2.

Reductive Half-Reaction of E_3(apoFeS). We investigated the kinetic properties of E_3(apoFeS), a form of E_3 from which the [2Fe-2S] center was removed by titration with mersalyl (see Materials and Methods). The reductive half-reaction of E_3(apoFeS) is kinetically simpler than that of E_3, and the results of these studies corroborate the steps proposed in the reaction mechanism of the holoenzyme detailed in Scheme 2. These studies were limited due to the relative instability of E_3(apoFeS). FAD was lost continuously during the course of the experiment, and attempts to reconstitute E_3(apoFeS, apoFAD) with FAD were unsuccessful. Approximate rates for the observed transitions are presented in Scheme 3. Figure 5 shows that the reductive half-reactions of E_3 and E_3(apoFeS) at 550 nm are nearly identical in the 5−100 ms time frame. Thus, the flavin reduction and NAD^+ release

Scheme 3: Reaction of E_3(apoFeS) with Reduced Pyridine Nucleotides[a]

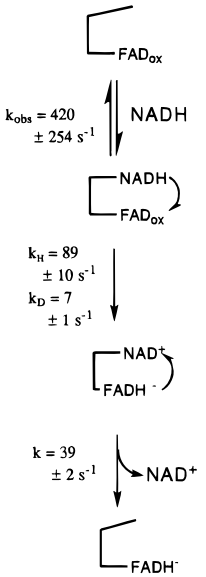

[a] Intermediate species are represented by stick diagrams; rate constants shown pertain to the reaction of 6 μM E_3(apoFeS) with 135 μM NADH.

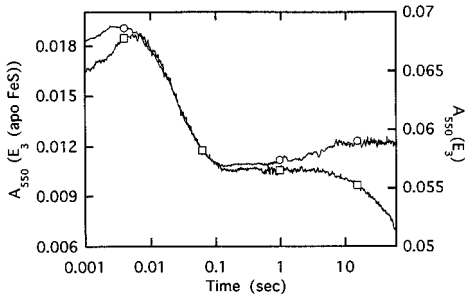

FIGURE 5: Comparison of the reactions of E_3 and E_3(apoFeS): (○) 6 μM E_3(apoFeS) and (□) 13 μM E_3 with 135 μM NADH at 4 °C in 50 mM phosphate buffer at pH 7.5.

steps of E_3(apoFeS) are very similar to those occurring in the reaction of holo-E_3 up to the step of [2Fe-2S] reduction. After about 1 s of reaction time, the 550 nm absorbance of holo-E_3 begins to decrease as the enzyme becomes fully reduced during an NADH-consuming disproportionation reaction. Since E_3(apoFeS) contains no iron−sulfur center, it cannot undergo this type of reaction. Thus, following the release of NAD^+, E_3(apoFeS) remains in the flavin hydroquinone state, and the absorbance at 550 nm remains nearly unchanged.

The reactions of E_3(apoFeS) with NADH or NADD are compared in Figure 6. The spectral changes and kinetic data obtained closely resemble those from the reaction of the holoenzyme (Figure 3). Apparently, the [2Fe-2S] center has little influence on the FAD reduction and NAD^+ release steps in the reductive half-reaction of E_3. The similar kinetic behavior of E_3 and E_3(apoFeS) is consistent with a structure in which the flavin and pyridine nucleotide binding domains are well-resolved from the [2Fe-2S] binding region.

pH Dependence of the Reductive Half-Reaction. In the reaction of E_3 with NADH, the steps of coenzyme binding, hydride transfer, and NAD^+ release (upper half of Scheme 2) are found to be quite independent of pH over the range of 6.5−10.0. The similarity between the kinetics of the formation and decay of the FAD and pyridine nucleotide

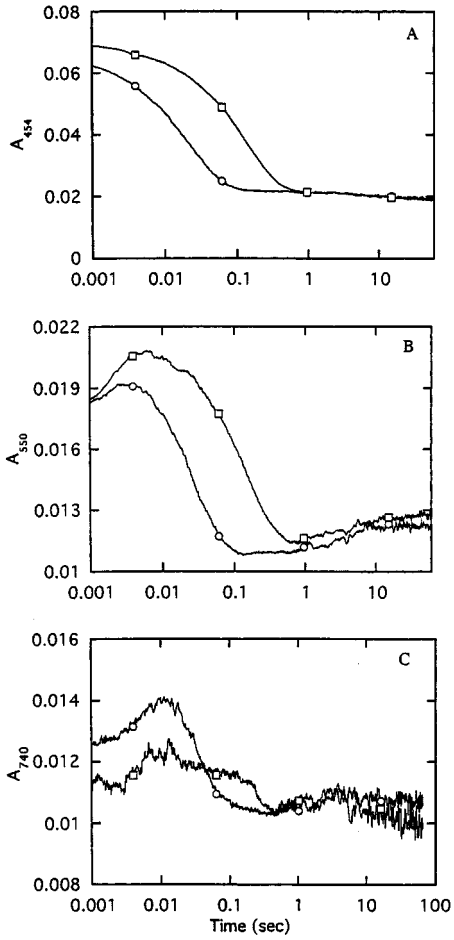

FIGURE 6: Deuterium isotope effect in the hydride transfer reaction of E_3(apoFeS). Comparison of the reaction of 6 μM E_3(apoFeS) with (○) 135 μM NADH or (□) 135 μM NADD at 4 °C in 50 mM phosphate buffer at pH 7.5.

charge transfer complexes at pH 7.0 and 10.0 observed at 725 nm is shown in Figure 7A. At both high and low pH values, intramolecular electron transfer is observed to occur as rapidly as NAD^+ is released from the enzyme. Following the release of NAD^+, free NADH, if present in solution, binds tightly to the two-electron-reduced E_3 (Figure 2). However, this binding does not appear to significantly alter the distribution of electrons between the FAD and the [2Fe-2S] center. Following the release of NAD^+ (lower half of Scheme 2), the extent of the intramolecular electron transfer from the flavin hydroquinone to the oxidized [2Fe-2S] center of E_3, which yields an enzyme containing neutral FAD semiquinone and a reduced [2Fe-2S] center, is highly dependent on pH (see the kinetic data collected from 50 ms to longer times in Figure 7A−C and spectra in Figure 8). At pH 7.0, intramolecular electron transfer is less favored; following the release of NAD^+, a significant fraction of the enzyme remains stabilized in the oxidized [2Fe-2S] and flavin hydroquinone state. At pH 10.0, intramolecular electron transfer gives a high yield of the reduced [2Fe-2S] and flavin semiquinone state, suggesting that the redox potential vs pH curve is more shallow for the [2Fe-2S] center than for the FAD moiety. Thus, at high pH values, the FAD_{sq}/FAD_{hq} redox potential is lower than that of the [2Fe-2S] center. The amount of semiquinone stabilized at various pH values was estimated from spectral data at 650 nm where the FAD semiquinone absorbs strongly, and the fully oxidized and reduced forms of E_3 have low and nearly equal absorbance (Figure 4). The amount of 650 nm absorbance following intramolecular electron transfer after 1 s plotted as a function of pH is presented in Figure 7D. A hyperbolic fit to this data gives a pK_a of 7.3 at 4 °C.

pH Jump Studies. In the reductive half-reaction of E_3, the steps of NAD^+ release and intramolecular electron transfer are observed as a single reaction phase, suggesting that the rate of electron transfer may be controlled by the dissociation of NAD^+. We were able to resolve the intramolecular electron transfer and NAD^+ release reactions by using double mixing stopped flow and pH jump methodology. In the first stage of mixing, E_3 was rapidly combined with excess NADH at either high or low pH. After 250 ms, hydride transfer and the dissociation of NAD^+ from the enzyme is complete. At this reaction time, the enzyme exists almost exclusively in the two-electron-reduced state, and the influence of the relatively slow bimolecular disproportionation reaction of E_3 molecules, which results in the formation of three-electron-reduced enzyme, is insignificant (Scheme 2, Figure 7). In the second stage of the experiment, the pH of the 250 ms reaction mixture was rapidly changed by mixing it with a buffer solution of either higher or lower pH, triggering a redistribution of electrons between the FAD and [2Fe-2S] centers.

Reactions following a jump of pH (pH 7.0 to 10.0 and pH 10.0 to 7.0) are presented in Figure 9. In the pH 7.0 to 10.0 jump, 78 μM E_3 was mixed in an Applied Photophysics Laboratories instrument with 1 mM NADH in 100 mM MOPS buffer at pH 7.0 and 22 °C. At 250 ms, this reaction mixture was mixed with 100 mM CAPS buffer containing excess KOH such that the pH of the final mixed buffer solution was 10.0. Since the double mixing experiment diluted the initial reactants by a factor of 4, the final concentration of E_3 participating in the pH jump reaction was 19.5 μM. In this reaction, a rapid increase in A_{650} of about 1300 s^{-1}, consistent with electron transfer from FAD_{hq} to the oxidized [2Fe-2S] center to form FAD_{sq} and $[2Fe\text{-}2S]_{red}$, was observed.

In the pH 10.0 to 7.0 jump, 78 μM E_3 was mixed with 1 mM NADH in the 100 mM CAPS buffer. After 250 ms, the reaction mixture was diluted with 100 mM MOPS buffer containing excess HCl such that the pH of the final mixed buffer solution was 7.0. In this reaction, a 220 s^{-1} decrease in absorbance occurs, indicative of electron transfer from the reduced [2Fe-2S] center to the FAD_{sq} to form FAD_{hq} and $[2Fe\text{-}2S]_{ox}$. Thus, it appears that, following the release of NAD^+, the equilibration of electrons between the [2Fe-2S] and FAD centers is rapid and that during turnover NAD^+ regulates the rate of electron transfer.

Photochemical Reduction. Photochemical reductions of E_3 conducted at pH 7.0 and 10.0 in the absence of pyridine nucleotides are shown in Figure 10A,B. These reactions occurred in two stages that are revealed by the difference spectra presented in Figure 10C,D. The first difference spectrum calculated at both low and high values of pH is consistent with the selective reduction of the [2Fe-2S] center of the enzyme. Subsequently, at high pH, the flavin moiety is reduced by two electrons without the intermediate formation of semiquinone. At low pH, the second stage of photoreduction involves the conversion of oxidized flavin to neutral flavin semiquinone as indicated by the negative difference absorption near 600−650 nm in Figure 10C. The

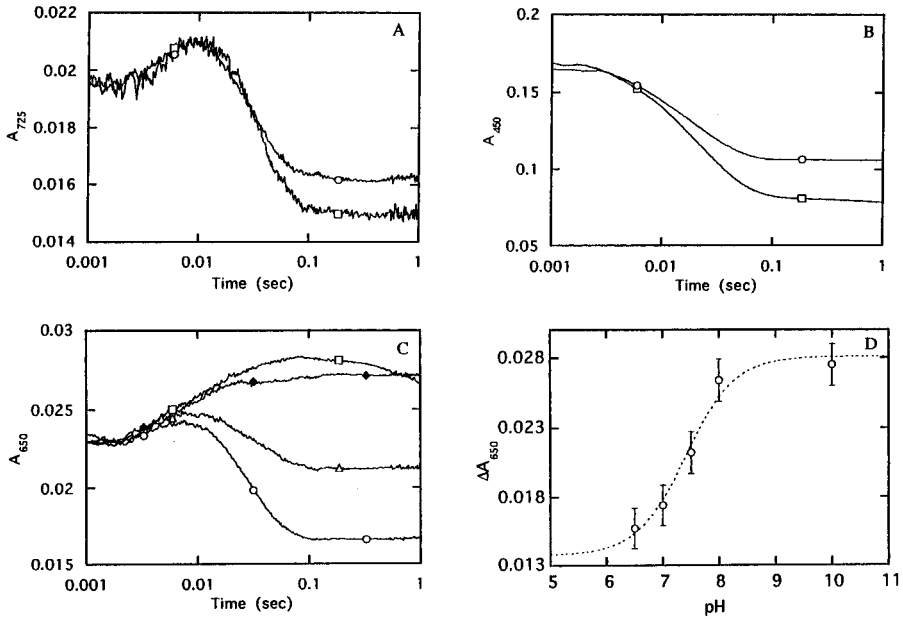

FIGURE 7: pH dependence of the reduction of E_3 by NADH. Reaction of 8.6 μM E_3 with 500 μM NADH at 4 °C in (○) 100 mM MOPS buffer at pH 7.0, (△) 100 mM TRIS buffer at pH 7.5, (◆) 100 mM TRIS buffer at pH 8.0, and (□) 100 mM CAPS buffer at pH 10.0. Data are compared at (A) 725 nm, (B) 450 nm, and (C) 650 nm. (D) Plot of the pH dependence of the absorbance change at 650 nm used to estimate the pK_a associated with semiquinone formation.

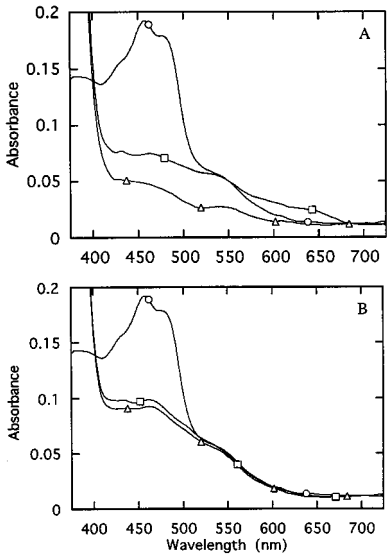

FIGURE 8: Spectra of the reduction of E_3 by NADH at pH 10 and 7. Spectra were recorded with a High-Tech stopped flow instrument by rapidly scanning the monochromator (200 nm s^{-1}): (A) 8.3 μM E_3 reacting with 500 μM NADH at pH 10.0 (○) before mixing with NADH, (□) 1−4 s after mixing, and (△) 790 s after mixing; and (B) 8.3 μM E_3 reacting with 500 μM NADH at pH 7.0 (○) before mixing with NADH, (□) 1−4 s after mixing with NADH, and (△) 606 s after mixing.

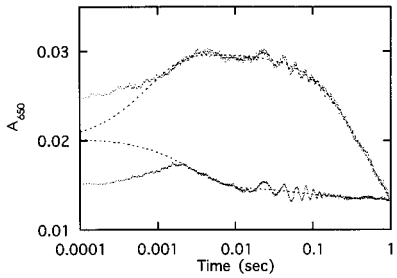

FIGURE 9: pH Dependence of the rate of intramolecular electron transfer in E_3. The plot shows fits (dashed lines) through data recorded in pH jump studies performed with the double-mixing stopped flow at 650 nm. The upper trace reflects the reaction that occurs in the pH 7.0 to 10.0 jump. The lower trace reflects the reaction that occurs in the pH 10.0 to 7.0 jump. See the text for further details.

neutral semiquinone could not be completely converted to the fully reduced state even after extended photoirradiation. These equilibrium redox states observed in the photochemical reactions are different from the intermediates observed in the reaction of E_3 with NADH following the release of NAD^+ (FAD_{hq} and $[2Fe\text{-}2S]_{ox}$ at pH 7.0; FAD_{sq} and $[2Fe\text{-}2S]_{red}$ at pH 10.0). This suggests that kinetic intermediate states of E_3 observed in the reductive half-reaction may differ in both their structural and their electronic properties from the states of E_3 that are stabilized at equilibrium. Exact redox potentials of the equilibrium states of E_3 are being investigated.

DISCUSSION

The interchange of hydride and single electron transfers catalyzed by NAD(P)H-dependent iron−sulfur flavoenzymes follows highly conserved chemistry and has been found in diverse biochemical pathways, such as photosynthesis, respiration, and oxidative catabolism (Karplus *et al.*, 1991; Correll *et al.*, 1992). These modular enzymes all have well-defined flavin and pyridine nucleotide binding domains, and they contain an additional flavin, [2Fe-2S], or cytochrome that is attached N-terminally or C-terminally or exists in a separate peptide. The conserved structure of the flavin and pyridine nucleotide binding domains relates all of these enzymes to the ferredoxin−NADP reductase (FNR) family of flavoenzymes (Karplus *et al.*, 1991; Correll *et al.*, 1992, 1993). Analysis of the primary sequence of E_3 has identified it as another member of the FNR family of flavoenzymes with a ferredoxin domain located at the N-terminus (Ploux *et al.*, 1995). With the addition of E_3 to the FNR family of iron−sulfur flavoenzymes, a novel biological conversion has been added to the repertoire of this rich and interesting class of proteins.

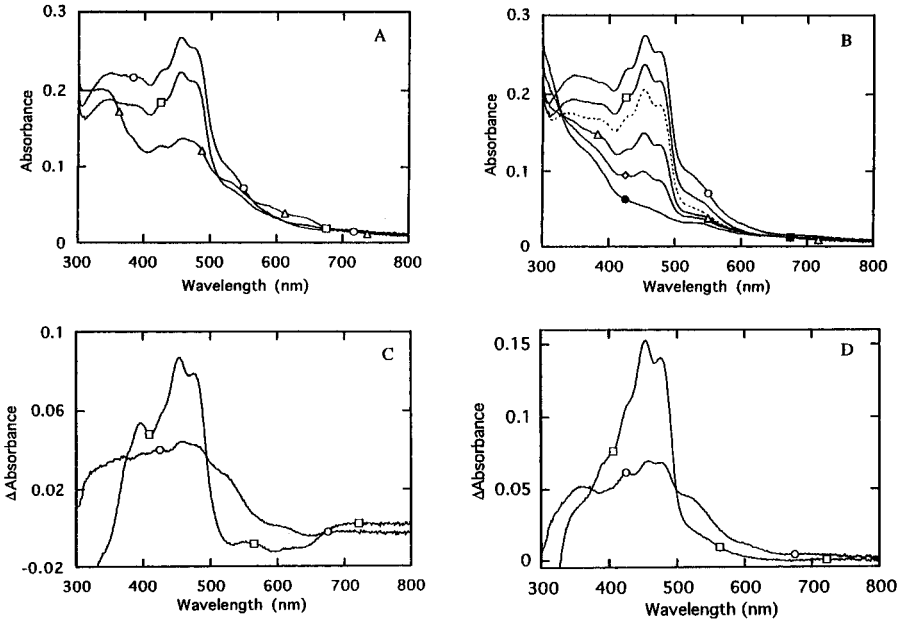

FIGURE 10: Photochemical reductions of E_3. Spectra of E_3 taken at pH 7.0 (A) (○) before and after (□) 7 min and (△) 14 min of photoirradiation with a 650 W tungsten lamp. (B) Spectra of E_3 taken at pH 10.0 (○) before and after (□) 1 min, (△) 2 min, (◇) 3 min, and (●) 6 min of photoirradiation and (- - -) after mixing in air. (C) Spectral differences between (○) oxidized and 7 min-photoreduced enzyme and (□) 7 min-photoreduced and 14 min-photoreduced enzyme at pH 7.0. (D) Spectral differences between (○) oxidized and air-reoxidized enzyme and (□) air-reoxidized and 6 min-photoreduced enzyme at pH 10.0.

Several steps characteristic of the reaction of flavoenzymes with pyridine nucleotides are found in the reductive half-reaction of E_3 (Scheme 2). NADH initially binds E_3 to form a charge transfer complex with the oxidized FAD moiety. A similar complex is observed in the reductive half-reaction of the closely related enzymes, phthalate dioxygenase reductase (PDR) (Gassner *et al*., 1994) and adrenodoxin reductase (Lambeth & Kamin, 1976), and in the oxidative half-reaction of FNR (Batie & Kamin, 1986). The assignment of this intermediate as a charge transfer complex between the oxidized FAD and the reduced nicotinamide ring of associated NAD(P)H is based on studies with model compounds and on the crystal structures of NAD(P)H-bound FNR (Pai *et al*., 1988), glutathione reductase, and PDR (Karplus *et al*., 1991; Correll *et al*., 1992, 1993). In E_3, the rate of formation of this complex increases linearly with NADH concentration, suggesting that it represents the initial Michaelis complex of NADH and the enzyme. This differs from the two-step mechanism observed in PDR, where PDR binds NADH in rapid equilibrium to form a Michaelis complex that has no charge transfer absorbance and then isomerizes to form the NADH and oxidized FMN charge transfer complex (CT-1) (Gassner *et al*., 1994). Thus, if a separate Michaelis complex does initially form in the reaction of E_3 with NADH, it must isomerize very rapidly to the observed charge transfer complex.

Following the binding of NADH, the absorbance increases at 725 nm and decreases at both 454 and 550 nm with a rate of 107.5 s^{-1} (Figures 1 and 4). These changes are consistent with hydride transfer and the conversion of the NADH and oxidized flavin charge transfer complex to an $NAD(P)^+$ and flavin hydroquinone charge transfer complex (Batie & Kamin, 1984; Gassner *et al*., 1995). The 10-fold deuterium isotope effect on this phase of the reaction confirms that it is indeed a hydride transfer step. A similar 7-fold effect is observed on the hydride transfer reaction of PDR (Gassner *et al*., 1994).

The absorbance decreases in the next two phases as the NAD^+ and FAD_{hq} charge transfer complex decomposes. The first phase of the decay, which occurs at 77.5 s^{-1}, may be due to an isomerization of enzyme structure that weakens the NAD^+-FAD_{hq} charge transfer interaction. In the second step, all charge transfer absorbance is lost at 42.5 s^{-1} as NAD^+ is released from the enzyme. The proposed isomerization step of this NAD^+ dissociation reaction is not observed in PDR where the release of NAD^+ occurs as a monophasic 35 s^{-1} decrease in charge transfer absorbance (Gassner *et al*., 1994).

Intramolecular, single electron transfer from the flavin hydroquinone to the oxidized [2Fe-2S] center of E_3 is observed to occur at the same rate at which NAD^+ is released from the enzyme, and the NAD^+ release rate is independent of solution pH. NAD^+ release also precedes electron transfer in the reductive half-reaction of PDR; it was proposed that intramolecular electron transfer is blocked until NAD^+ is released from the enzyme (Gassner *et al*., 1994; Gassner & Ballou, 1995). Similarly, in the reaction catalyzed by a related iron−sulfur flavoenzyme, trimethylamine dehydrogenase (TMADH), intramolecular electron transfer appears to be prohibited until product dissociates (Singer *et al*., 1980; Steenkamp & Beinert, 1982). Thus, in these enzymes, it appears that the intramolecular electron transfer from the flavin to the iron center may be triggered by the release of reaction products, probably through some small structural change.

Immediately following the release of NAD^+, excess NADH in solution binds tightly to the two-electron-reduced form of E_3. The formation of this complex, which results in a slight attenuation of the enzyme absorbance at 500 nm and longer wavelengths, poises the enzyme for subsequent hydride transfer. A similar complex of NADH with two-electron-reduced enzyme has been reported for the iron−sulfur flavoenzyme PDR (Gassner *et al*., 1994).

The extent of the intramolecular electron transfer reaction from the FAD_{hq} to the [2Fe-2S] center in E_3 is prototropically controlled by an ionizable group with a pK_a of about 7.3 (Figure 7D). On the basis of the pH-dependent distribution of electrons between the [2Fe-2S] and FAD centers of E_3, it can be concluded that at low pH the FAD_{sq}/FAD_{hq} couple is more positive than the $[2Fe\text{-}2S]_{ox}/[2Fe\text{-}2S]_{red}$ couple, since a spectrum consistent with a FAD_{hq} and oxidized [2Fe-2S] center is observed following the release of NAD^+ (see Figure 8B). However, at pH 10.0, immediately following the release of NAD^+, an enzyme spectrum consistent with FAD_{sq} and a reduced [2Fe-2S] center is observed (see Figure 8A). Accordingly, at high pH, the midpoint potential of the FAD_{sq}/FAD_{hq} couple is lower than that of the $[2Fe\text{-}2S]_{ox}/[2Fe\text{-}2S]_{red}$ couple, resulting in an increase in the extent of the intramolecular electron transfer from the FAD_{hq} to the oxidized [2Fe-2S] center following dissociation of NAD^+. Flavin hydroquinones are frequently ionized at position N-1 when they are bound to flavoenzymes (Müller *et al*., 1987); it was recently suggested that the protonation state of the N-1 position of the 6-cysteinyl-FMN moiety of trimethylamine dehydrogenase plays a key role in the regulation of electron transfer from the FMN to the [4Fe-4S] of this enzyme (Rohlfs *et al*., 1995). Similarly, the pK_a of 7.3 associated with the prototropic control of electron transfer in E_3 may represent the ionization state of the N-1 position of the FAD in this enzyme.

The two-electron-reduced E_3 maintains a neutral blue semiquinone after intramolecular electron transfer with no evidence for the formation of red flavin semiquinone anion, even at pH 10.0. Red semiquinone would exhibit strong absorbance near 380 nm and would have essentially no absorbance at wavelengths longer than 540 nm (Massey & Palmer, 1966). Neutral and anionic forms of free flavin semiquinone are related by reversible ionization at the N-5 position of the isoalloxazine ring system, which has a pK_a of about 8.3. However, it is not uncommon to find substantial shifts in the pK_a of the flavin semiquinone when the flavin is bound in the context of a specific protein environment (Müller, 1991). For instance, a hydrogen-bonding interaction at the N-5 position of the FMN in flavodoxin is thought to stabilize the blue semiquinone form of this enzyme at high pH (Ludwig *et al*., 1990). Similarly, the flavin of E_3 appears to resist ionization of N-5 to yield an anionic red semiquinone at high pH; consequently, the pK_a of the N-5 position of FAD bound to E_3 is probably greater than 10.

The transient distribution of electrons between the iron and flavin centers of E_3 observed following the release of NAD^+ during the reductive half-reaction at pH 7.0 or 10.0 is different from that found at equilibrium following the photochemical reduction of E_3 at the same pH values. Since the photochemical reductions exclude pyridine nucleotide, it was initially postulated that bound NADH could modulate the redox potential of the FAD moiety. It has been shown in some cases that binding of pyridine nucleotides affects flavin midpoint potentials (Lambeth & Kamin, 1976). However, there is no evidence for this in E_3. As the concentration of NADH is varied from stoichiometric to superstoichiometric, the concentration of flavin semiquinone observed following the release of NAD^+, penultimate to the disproportionation reaction, remains nearly constant. Thus, it appears that the thermodynamically and kinetically stabilized intermediates may have unique redox properties.

In order to distinguish the kinetically stabilized states of E_3, it was necessary to perform the pH jump studies using the double mixing stopped flow instrument. Under conditions free of the influence of bound NAD^+, the measured rates of intramolecular electron transfer from reduced FAD to the [2Fe-2S] center of E_3 at pH 7.0 or 10.0 are quite similar to those reported for the related enzyme, trimethylamine dehydrogenase (TMADH). In the latter enzyme, intramolecular electron transfer from 6-cysteinyl-FMN to the [4Fe-4S] cluster is controlled by the protonation state of one of the three ionizable groups (p$K_{a1} \sim 6.0$, p$K_{a2} \sim 8.0$, and p$K_{a3} \sim 9.5$) (Rohlfs *et al*., 1995; Rohlfs & Hille, 1991).

In contrast to those of the TMADH and E_3 systems, the rate of hydride transfer (from NADH to the FMN moiety) in PDR is sensitive to pH (p$K_a \sim 7.8$) (G. Gassner, unpublished results). The subsequent steps of NAD^+ release and intramolecular electron transfer in PDR are relatively pH-independent. The equilibrium distribution of electrons between the flavin and iron center that develops as a result of the intramolecular electron transfer also remains unperturbed in PDR under different pH conditions. Thus, variation in pH can have quite distinct effects on these iron−sulfur flavoenzymes despite their structural and mechanistic similarities.

The characteristic modular domain structure of the iron−sulfur flavoenzymes in the FNR family makes them particularly good subjects for studies of the function of individual domains and their interactions. The fact that the reductive half-reaction of E_3(apoFeS) closely parallels that of the holoenzyme up to the point of intramolecular electron transfer strongly suggests that the [2Fe-2S] center has little effect on the reaction kinetics of the flavin domain of E_3 with pyridine nucleotides. Similarly, the reductive half-reactions of PDR and PDR(−FeS), a truncated form of PDR that lacks an iron−sulfur domain, are nearly the same up to the point of intramolecular electron transfer (Gassner & Ballou, 1995). Thus, it may be concluded that the flavin and pyridine nucleotide binding domains of these systems remain functional even in the absence of a catalytically competent [2Fe-2S] center.

This work has concentrated on the electron transfer reactions involved with E_3 and its interactions with pyridine nucleotides. Since its redox partner, the E_1 enzyme, which contains a [2Fe-2S] center and a pyridoxamine cofactor, is intimately involved in the redox reactions of E_3 during normal catalysis, it is relevant to consider how bound E_1 might alter the redox properties of E_3, including intramolecular electron transfer. Studies are well under way on the complete system. It is found that, while in complex, the individual cofactor units act largely as they do independently, except, of course, for the intermolecular electron transfers. This work will be reported in considerable detail in separate publications about the redox potentials and about the kinetics and spectral properties.

ACKNOWLEDGMENT

The authors thank Dr. M. J. Coon for the use of the Cary 3E spectrophotometer, Dr. R. Neubig for the use of the Applied Photosystems stopped flow instrument, and Dr. V. Massey for the 5-deazariboflavin used in the photoreduction studies.

REFERENCES

Barshop, B. A., Wrenn, R. F., & Frieden, C. (1983) *Anal. Biochem. 130*, 134−145.

Batie, C. J., & Kamin, H. (1984) *J. Biol. Chem. 259*, 11976−11985.

Batie, C. J., & Kamin, H. (1986) *J. Biol. Chem. 261*, 11214−11223.

Bull, C., & Ballou, D. P. (1981) *J. Biol. Chem. 256*, 12673−12680.

Correll, C. C., Batie, C. J., Ballou, D. P., & Ludwig, M. L. (1992) *Science 258*, 1604−1610.

Correll, C. C., Ludwig, M. L., Bruns, C. M., & Karplus P. A. (1993) *Protein Sci. 12*, 2112−2133.

Gassner, G., & Ballou, D. P. (1995) *Biochemistry 34*, 13460−13471.

Gassner, G., Wang, L., Batie, C., & Ballou, D. P. (1994) *Biochemistry 33*, 12184−12193.

Gonzalez-Porqúe, P., & Strominger, J. L. (1972) *J. Biol. Chem. 247*, 6748−6756.

Griffiths, A. J., & Davies, D. B. (1991a) *Carbohydr. Polym. 14*, 241−279.

Griffiths, A. J., & Davies, D. B. (1991b) *Carbohydr. Polym. 14*, 339−365.

Grisebach, H. (1978) *Adv. Carbohydr. Chem. Biochem. 35*, 81−126.

Han, O., Miller, V. P., & Liu, H.-w. (1990) *J. Biol. Chem. 265*, 8033−8041.

Health, E. C., & Elbein, A. D. (1962) *Proc. Natl. Acad. Sci. U.S.A. 48*, 1209−1216.

Karplus, P. A., Daniels, M. J., & Herriott, J. R. (1991) *Science 258*, 1604−1610.

Kessler, A. C., Haase, A., & Reeves, R. R. (1993) *J. Bacteriol. 175*, 1412−1422.

Lambeth, J. D., & Kamin, H. (1976) *J. Biol. Chem. 251*, 4299−4306.

Lindberg, B. (1990) *Adv. Carbohydr. Chem. Biochem. 48*, 279−318.

Liu, H.-w., & Thorson, J. S. (1994) *Annu. Rev. Microbiol. 48*, 223−256.

Lo, S. F., Miller, V. P., Lei, Y., Thorson, J. S., Liu, H.-w., & Schottel, J. L. (1994) *J. Bacteriol. 176*, 460−468.

Lüderitz, O., Staub, A. M., & Westphal, O. (1966) *Bacteriol. Rev. 30*, 192−248.

Ludwig, M. L., Schopfer, L. M., Metzger, A. L., Pattridge, K. A., & Massey, V. (1990) *Biochemistry 29*, 10364−10375.

Massey, V., & Palmer, G. (1966) *Biochemistry 5*, 3181−3189.

Massey, V., & Hemmerich, P. (1977) *J. Biol. Chem. 252*, 5612−5614.

Massey, V., & Hemmerich, P. (1978) *Biochemistry 17*, 9−17.

Matsuhashi, S., Matsuhashi, M., & Strominger, J. L. (1966) *J. Biol. Chem. 241*, 4267−4274.

Miller, V. P., Thorson, J. S., Ploux, O., Lo, S. F., & Liu, H.-w. (1993) *Biochemistry 32*, 11934−11942.

Müller, F. (1991) *Chemistry & Biochemistry of Flavoenzymes*, pp 25−28, CRC Press, Boca Raton, FL.

Müller, F., Vervoort, J., van Mierlo, C. P. M., Mayhew, S. G., van Berkel, W. J. H., & Bacher, A. (1987) in *Flavins and Flavoproteins* (Edmundson, D. E., & McCormick, D. B., Eds.) pp 261−270, Walter de Gruyter & Co., Berlin.

Ovodov, Y. S., Gorshkova, R. P., Tomshich, S. V., Komandrova, N. A., & Zubkov, V. A. (1992) *J. Carbohydr. Chem. 11*, 21−35.

Pai, E., Karplus, P. A., & Schultz, G. E. (1988) *Biochemistry 27*, 4465−4474.

Ploux, O., Lei, Y., Vatanen, K., & Liu, H.-w. (1995) *Biochemistry 34*, 4159−4168.

Rohlfs, R. J., & Hille, R. (1991) *J. Biol. Chem. 266*, 15244−15252.

Rohlfs, R. J., Huang, L., & Hille, R. (1995) *J. Biol. Chem. 270*, 22196−22207.

Rubenstein, P. A., & Strominger, J. L. (1974a) *J. Biol. Chem. 249*, 3776−3781.

Rubenstein, P. A., & Strominger, J. L. (1974b) *J. Biol. Chem. 249*, 3782−3788.

Shibaev, V. N. (1986) *Adv. Carbohydr. Chem. Biochem. 44*, 277−339.

Singer, T. P., Steenkamp, D. J., Kenney, W. C., & Bienert, H. (1980) in *Flavins & Flavoproteins* (Yagi, K., & Yamano, T., Eds.) pp 277−287, Japan Scientific Societies Press, Tokyo.

Steenkamp, D. J., & Beinert, H. (1982) *Biochem. J. 207*, 241−252.

Thorson, J. S., & Liu, H.-w. (1993a) *J. Am. Chem. Soc. 115*, 7539−7540.

Thorson, J. S., & Liu, H.-w. (1993b) *J. Am. Chem. Soc. 115*, 12177−12178.

Weigel, T. M., Liu, L., & Liu, H.-w. (1992a) *Biochemistry 31*, 2129−2139.

Weigel, T. M., Miller, V. P., & Liu, H.-w. (1992b) *Biochemistry 31*, 2140−2147.

Yu, Y., Russell, R. N., Thorson, J. S., Liu, L.-d., & Liu, H.-w. (1992) *J. Biol. Chem. 267*, 5868−5875.

Zimmerele, C. T., & Frieden, C. (1989) *Biochem. J. 258*, 381−387.

BI960217Z